KLF6-SV1 overexpression accelerates human and mouse prostate cancer progression and metastasis

Goutham Narla,[1,2] Analisa DiFeo,[1] Yolanda Fernandez,[1] Saravana Dhanasekaran,[3] Fei Huang,[1] Jaya Sangodkar,[1,2] Eldad Hod,[2] Devin Leake,[4] Scott L. Friedman,[2] Simon J. Hall,[5] Arul M. Chinnaiyan,[3] William L. Gerald,[6] Mark A. Rubin,[7] and John A. Martignetti[1,8]

[1]Department of Genetics and Genomic Sciences and [2]Department of Medicine, Mount Sinai School of Medicine, New York, New York, USA. [3]Department of Pathology, University of Michigan Medical School, Ann Arbor, Michigan, USA. [4]Thermo Fisher Scientific, Lafayette, Colorado, USA. [5]Department of Urology, Mount Sinai School of Medicine, New York, New York, USA. [6]Department of Pathology, Memorial Sloan-Kettering Cancer Center, New York, New York, USA. [7]Department of Pathology, Brigham and Women's Hospital, Harvard Medical School, Boston, Massachusetts, USA. [8]Department of Oncological Sciences, Mount Sinai School of Medicine, New York, New York, USA.

Metastatic prostate cancer (PCa) is one of the leading causes of death from cancer in men. The molecular mechanisms underlying the transition from localized tumor to hormone-refractory metastatic PCa remain largely unknown, and their identification is key for predicting prognosis and targeted therapy. Here we demonstrated that increased expression of a splice variant of the Kruppel-like factor 6 (*KLF6*) tumor suppressor gene, known as *KLF6-SV1*, in tumors from men after prostatectomy predicted markedly poorer survival and disease recurrence profiles. Analysis of tumor samples revealed that *KLF6-SV1* levels were specifically upregulated in hormone-refractory metastatic PCa. In 2 complementary mouse models of metastatic PCa, KLF6-SV1–overexpressing PCa cells were shown by in vivo and ex vivo bioluminescent imaging to metastasize more rapidly and to disseminate to lymph nodes, bone, and brain more often. Interestingly, while KLF6-SV1 overexpression increased metastasis, it did not affect localized tumor growth. *KLF6-SV1* inhibition using RNAi induced spontaneous apoptosis in cultured PCa cell lines and suppressed tumor growth in mice. Together, these findings demonstrate that KLF6-SV1 expression levels in PCa tumors at the time of diagnosis can predict the metastatic behavior of the tumor; thus, KLF-SV1 may represent a novel therapeutic target.

Introduction

Metastatic prostate cancer (PCa) is a leading cause of cancer death in men. More than 234,460 men were predicted to be diagnosed with PCa in 2007, and 27,350 were expected to die from the disease (1). While the aggressive use of prostate-specific antigen (PSA) testing has been effective in detecting PCa at earlier stages of the disease, one of the major limitations is the inherent clinical heterogeneity of PCa. Specifically, clinically significant and insignificant PCa cells are not always distinguishable at the time of diagnosis. Ultimately, a number of patients with apparently localized disease will succumb to PCa despite radical prostatectomy. The identification of molecular markers and pathways that can accurately predict PCa risk and distinguish between indolent cancer cells and those with a greater metastatic potential are essential for future effective management and treatment decisions and for defining potential therapeutic targets.

Accumulating evidence suggests that the tumor suppressor gene Kruppel-like factor 6 (*KLF6*; also known as *COPEB* and *ZF9*) and its dominant-negative splice form *KLF6-SV1* play an important role in both the development and the progression of cancer (refs. 2–15 and our unpublished observations). Intriguingly, a number of genomic studies have identified KLF6 and KLF6-SV1 expression as part of a multigene signature that can define clinical outcome in PCa (11, 12) or its development and chemoresistance in other cancers (8, 9, 13). In particular, these data — combined with previous studies linking increased KLF6-SV1 expression with an increased lifetime risk of PCa (14), demonstrating its overexpression in prostate tumors (14), and identifying a role for KLF6-SV1 in the regulation of key cancer-relevant pathways including apoptosis, angiogenesis, cellular migration/invasion, and proliferation — make KLF6-SV1 an attractive candidate gene for risk prognostication and therapy (refs. 14, 15, and our unpublished observations). However, the precise role of KLF6-SV1 in regulating the metastatic process in vivo, its expression pattern and prognostic utility in PCa specimens, and its therapeutic potential remain largely unknown. The present studies were directed toward exploring the biological relevance of KLF6-SV1 to PCa progression and metastasis and functional consequences of targeted reduction of KLF6-SV1 using RNAi in PCa models. Our findings suggest that KLF6-SV1 expression levels at the time of prostatectomy can predict disease recurrence risk. In addition, in vivo studies in mice revealed that overexpression of KLF6-SV1 in tumor cells allows tumors to metastasize more rapidly to lymph nodes, bones, and brain. Thus, KLF6-SV1 may represent a novel therapeutic target for inhibiting metastasis in prostate cancer.

Nonstandard abbreviations used: BLI, bioluminescent imaging; BPH, benign prostatic hyperplasia; KLF6, Kruppel-like factor 6; PCa, prostate cancer; PCNA, proliferating cell nuclear antigen; qRT-PCR, quantitative real-time PCR; si-NTC, nontargeting control siRNA; si-SV1, KLF6-SV1–specific siRNA.

Conflict of interest: Oncomine, which was used in this study, is freely available to the academic community. The University of Michigan has licensed the commercial rights to Oncomine to Compendia Biosciences Inc., which was cofounded by A.M. Chinnaiyan. M.A. Rubin and A.M. Chinnaiyan serve as consultants to Gen-Probe. Gen-Probe has not played a role in the design and conduct of the study; in the collection, analysis, or interpretation of the data; or in the preparation, review, or approval of the manuscript.

Citation for this article: *J. Clin. Invest.* **118**:2711–2721 (2008). doi:10.1172/JCI34780.

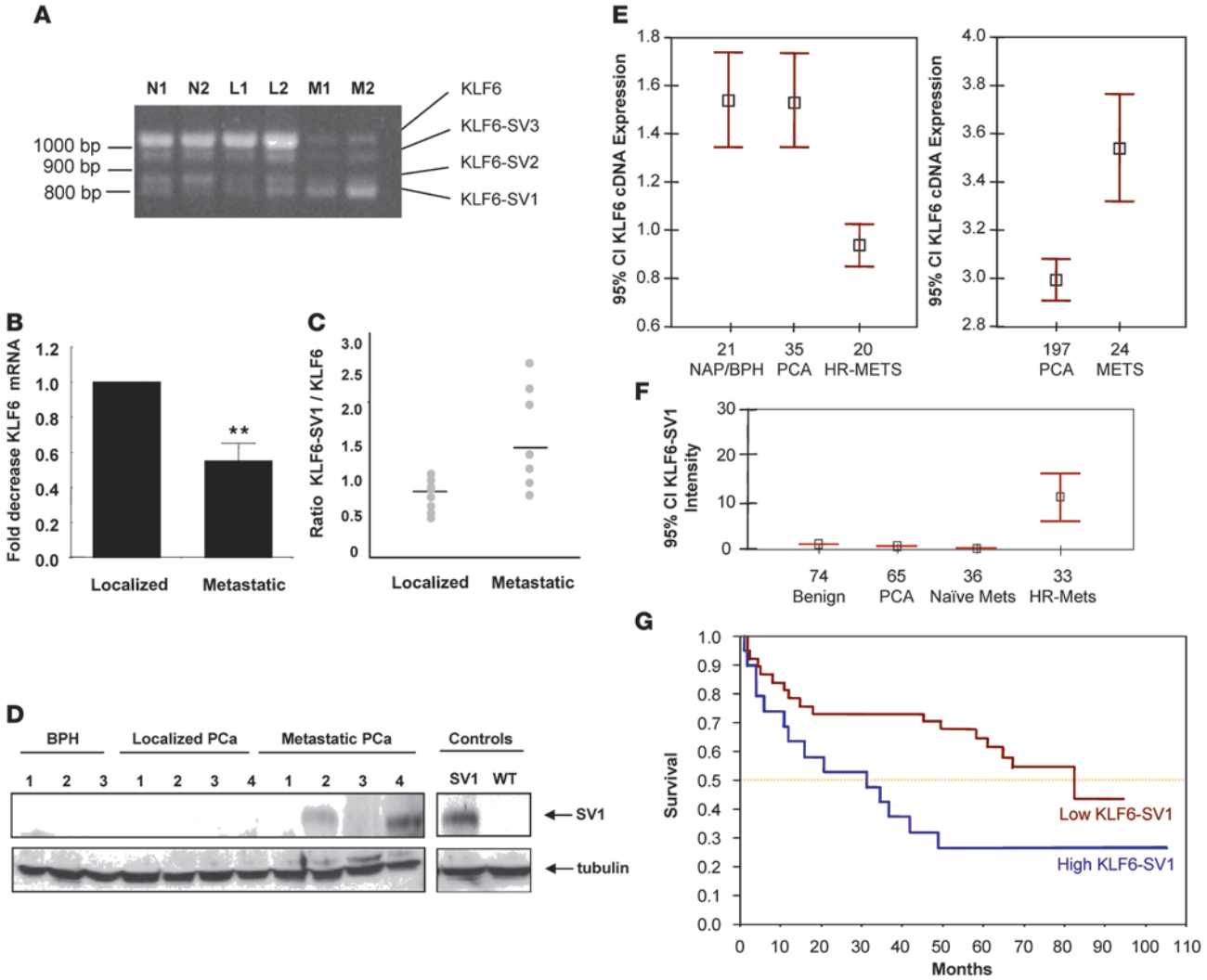

Figure 1

Expression of KLF6 and its splice variants in PCa. (**A**) RT-PCR of representative prostate-derived cDNAs with KLF6-specific primers. N, normal prostate; L, localized PCa; M, metastatic PCa. (**B**) qRT-PCR analysis of localized and metastatic PCa cDNAs for wild-type KLF6 expression. Metastatic tumors expressed significantly less wild-type KLF6 mRNA compared with localized tumors. $^{**}P < 0.001$. (**C**) qRT-PCR of localized and metastatic PCa samples using wild-type KLF6– and KLF6-SV1–specific PCR primers (refs. 14, 15, and our unpublished observations). (**D**) Increased KLF6-SV1 expression in metastatic PCa. Western blot analysis using a KLF6-SV1–specific monoclonal antibody (ref. 15 and our unpublished observations). Transfected KLF6-SV1 and transfected wild-type KLF6 controls were run on the same gel but were noncontiguous. Tubulin was used as the loading control for all lanes. (**E**) Left: DNA microarray analysis of PCa demonstrated downregulation of KLF6 mRNA in hormone-refractory metastatic PCa (HR-MET) compared with both noncancerous prostate tissue and localized PCa. NAP, normal adjacent prostate tissue; PCA, localized PCa. Right: Tissue microarray analysis of KLF6 expression using KLF6 monoclonal antibody 2A2. Data points and error bars represent mean KLF6 protein expression and 95% confidence intervals, respectively. (**F**) Immunohistochemistry of high-density tissue microarray analyses with the KLF6-SV1–specific monoclonal antibody demonstrated marked upregulation of KLF6-SV1 expression in hormone-refractory metastatic PCa compared with naive metastatic PCa, localized PCa, and benign prostate tissue ($P < 0.001$). Data points and error bars represent mean KLF6-SV1 protein expression and 95% confidence intervals, respectively. (**G**) Median survival, as measured using biochemical recurrence and assessed by qRT-PCR, in men whose localized prostate tumors expressed high levels of KLF6-SV1 (blue) was 30 mo compared with 80 mo in men with low KLF6-SV1–expressing tumors ($P < 0.01$).

Results

KLF6 and KLF6-SV1 are differentially expressed in localized and metastatic PCa. We initially carried out RT-PCR of cDNA derived from a discovery set of tissues representing normal, localized, and metastatic PCa samples. The metastatic tissue expression pattern was unique in that it demonstrated a marked decrease in the full-length tumor suppressor KLF6 with relative overexpression of the KLF6 splice variants KLF6-SV1, KLF-SV2, and KLF-SV3 (Figure 1, A and B). Quantitative real-time PCR (qRT-PCR) analysis of localized and metastatic PCa–derived cDNA confirmed that whereas wild-type KLF6 levels significantly decreased in metastatic tumors, a subset of these tumors (3 of 7) had markedly increased ratios of KLF6-SV1 to KLF6 expression (Figure 1C). Protein extracts from a subset of normal, localized, and metastatic cancer tissues were then immunoblotted using the KLF6

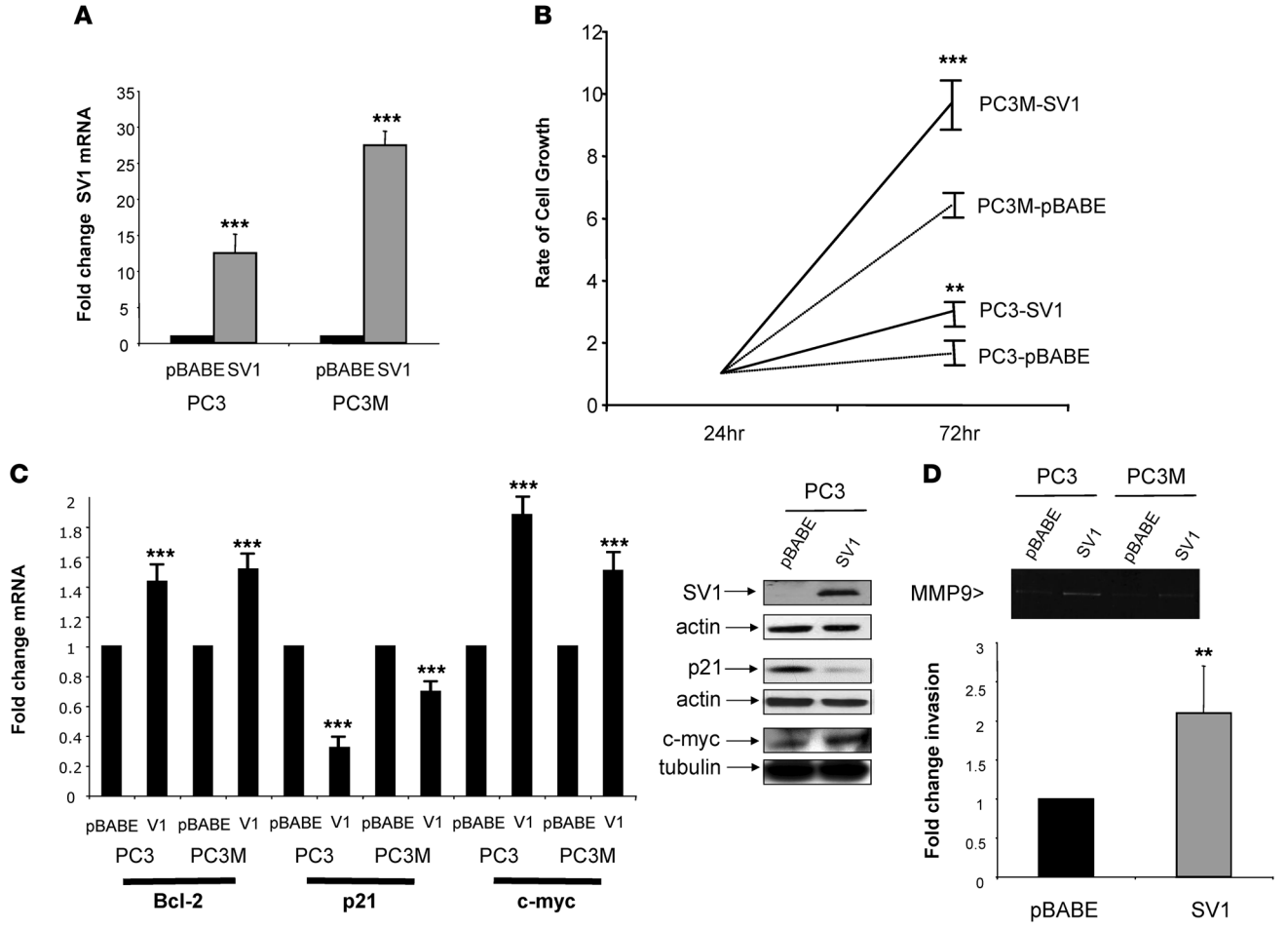

Figure 2

Overexpression of KLF6-SV1 in PCa cell lines. (**A**) qRT-PCR analysis of pBABE and KLF6-SV1 vector–retrovirally infected PC3 and P3M cell lines demonstrated 12- and 27-fold overexpression, respectively, of KLF6-SV1 in pBABE-SV1 vector–infected cell lines compared with control. (**B**) KLF6-SV1–overexpressing cell lines proliferated significantly more than control cell lines, assessed by tritiated thymidine incorporation at 24 and 72 h of the PC3 and PC3M cell lines. Mean change in cell growth rate from 3 independent experiments is shown. (**C**) Increased expression of the oncogene c-myc and antiapoptotic Bcl-2, with concomitant reduction of the cyclin-dependent inhibitor p21, in KLF6-SV1–expressing cell lines. RNA and protein were harvested from 3 independent experiments, and qRT-PCR and Western blotting were performed. Overexpression of KLF6-SV1 increased Bcl-2 expression 50%, increased c-myc expression 80%, and reduced p21 expression 50% in PCa cell lines at the mRNA and protein levels. Actin was used as loading control for KLF6-SV1 and p21; tubulin was used for c-myc. (**D**) Increased invasion in KLF6-SV1 cell lines was associated with increased expression of MMP9. Gelatin zymography of the supernatant isolated from PC3 and PC3M cell lines is shown. Overexpression of KLF6-SV1 increased MMP9 expression in both PC3 and PC3M lines. KLF6-SV1–expressing stable PC3 cell lines (PC3-SV1) were 2-fold more invasive through a Matrigel basement membrane. The number of invasive cells was counted from 4 fields from 3 independent experiments. $^{**}P < 0.01$, $^{***}P < 0.001$ versus control.

monoclonal antibody 2A2, which recognizes all KLF6 protein products including KLF6-SV1 (14, 15). KLF6-SV1 protein was present in metastatic tumors (2 of 4), but was not detectable in either benign prostatic hyperplasia (BPH; 0 of 3) or localized PCa samples (0 of 4; Figure 1D). In each of these assays, KLF6-SV2 and KLF6-SV3 expression levels were not markedly affected (data not shown).

These results suggested that decreased KLF6 expression and KLF6-SV1 overexpression were associated features of tumor metastasis. Therefore, we analyzed KLF6 gene and protein expression profiles in additional, larger sample sets. First, we examined a set containing 76 patient-derived samples using a 9,984-element (10K) human cDNA microarray. In this set, we compared benign prostate tissue ($n = 21$), clinically localized PCa ($n = 35$), and metastatic prostate tumors ($n = 20$) (16). Using a significance analysis of microarray test, overall KLF6 expression (because the probe used detects all family members) was downregulated 1.64-fold in metastatic tissue compared with localized tumor and nonmalignant BPH tissue samples ($P < 0.0001$, 1-way ANOVA; Figure 1E).

Second, PCa tissue samples from 197 clinically localized tumors and 24 hormone-refractory prostate tumors were examined by immunohistochemistry for KLF6 protein expression using the KLF6 monoclonal antibody 2A2. Unexpectedly, given the decrease seen in overall KLF6 gene expression, there was an increase in cytoplasmic staining in metastatic versus localized prostate tumor samples ($P < 0.001$; Figure 1E). Given our finding of increased KLF6-SV1 expression in metastatic prostate tumors (Figure 1, C and D) and the fact that this

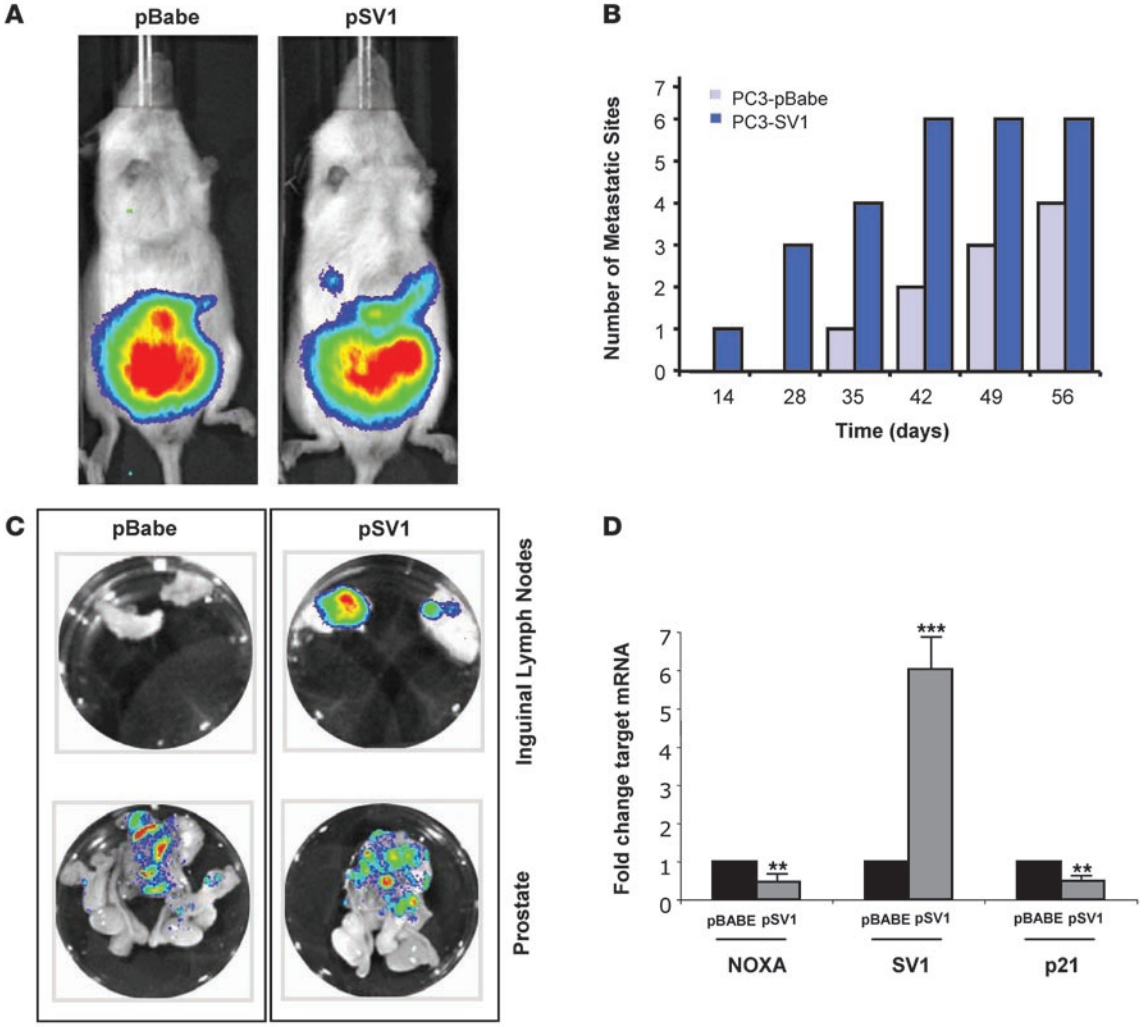

Figure 3

Overexpression of KLF6-SV1 in an orthotopic mouse model of PCa progression results in increased metastasis. (**A**) Male SCID beige mice were anesthetized, and the dorsolateral aspect of the prostate was injected with 1×10^6 PC3 cells in 25 μl PBS. Tumors were imaged every week to determine local tumor growth and evidence of tumor cell dissemination. A representative image of 2 mice is illustrated. Local tumor growth, as determined by fluorescent intensity, was equal between control and KLF6-SV1 mice. (**B** and **C**) KLF6-SV1–overexpressing cells metastasized more frequently than did control cells. The number of metastatic lesions was determined using a combination of whole-body imaging and ex vivo histological analysis of all mice upon sacrifice (n = 8 [pBABE]; 9 [pSV1]); representative images of ex vivo tissue analysis are shown. (**D**) pSV1 vector–derived tumors expressed significantly less NOXA and p21 than did control tumors. qRT-PCR of pSV1 vector–derived tumors using real-time primers specific to NOXA, KLF6-SV1, and p21 demonstrated marked overexpression of KLF6-SV1 in pSV1 vector–derived tumors with concomitant reduction in p21 and NOXA expression. $^{**}P < 0.01$, $^{***}P < 0.001$ versus control.

isoform lacks an NLS sequence (14), we hypothesized that increased KLF6-SV1 cytoplasmic expression was responsible for this overall increase. To refine this analysis, we used a KLF6-SV1–specific monoclonal antibody in tissue microarrays containing normal prostate tissue, BPH, localized PCa, and hormone-refractory metastatic PCa specimens. Consistent with our hypothesis, while overall expression of all KLF6 family members decreased with PCa progression, KLF6-SV1 expression was specifically and significantly increased in hormone-refractory metastases (Figure 1F).

Increased KLF6-SV1 predicts poor survival in men with localized PCa. Having identified this isoform-specific increase in late-stage disease, we next sought to determine whether KLF6-SV1 expression in localized PCa is associated with disease recurrence and poor survival. qRT-PCR using KLF6-SV1–specific primers (14, 15) was performed on an independent cohort of 61 primary prostate tumors with associated clinicopathological correlates, including disease-free survival. In these studies, biochemical recurrence was used to generate the survival function. Univariate and multivariate analysis adjusting for tumor stage and Gleason score revealed that increased KLF6-SV1 expression was strongly associated with poor survival. The median survival difference was greater than 4 years. Patients with high levels of KLF6-SV1 expression had a median survival of approximately 30 months, compared with 80 months in patients with low KLF6-SV1 expression ($P < 0.01$; Figure 1G).

KLF6-SV1 overexpression increases cellular proliferation and invasion. To extend our clinical studies and determine the biological rel-

Table 1
KLF6-SV1–overexpressing cells metastasize more frequently than do control cells

	pBABE	pBABE-SV1
Lymph node	18%	45%[A]
Visceral organ	5%[A]	22%[A]
Total metastases	24%	62%[A]

The number of metastatic lesions was determined using a combination of whole-body imaging and ex vivo histological analysis of all mice upon sacrifice (n = 8 [pBABE]; 9 [pSV1]). Values represent tumor incidence. [A]$P < 0.01$.

evance of these findings based on examination of nearly 600 patient-derived samples in total, we generated stable cell lines overexpressing KLF6-SV1 in 2 related PCa cell lines: PC3 and its metastatic derivative, PC3M (2). Interestingly, the PC3M line expressed substantially higher levels of KLF6-SV1 mRNA and protein than did the parental PC3 cell line (data not shown). Retroviral infection resulted in 10- to 30-fold overexpression of KLF6-SV1 mRNA and protein in each compared with pBABE vector–infected control cell lines (Figure 2A). Overexpression increased cellular proliferation by 50% and 95% in the PC3 and PC3M cell lines, respectively (Figure 2B).

Using known KLF6-regulated targets and pathways (refs. 14, 15, 17–20, and our unpublished observations) as a guide, we analyzed the expression profile of a number of target genes in both cell lines. KLF6-SV1 overexpression resulted in downregulation of the cyclin-dependent kinase inhibitor p21 and upregulation of a number of genes, including the prosurvival gene Bcl-2 and the oncogene c-myc (Figure 2C). In addition, the metalloproteinase MMP9, which has been closely linked to tumor cell migration and invasion, was also overexpressed (Figure 2D). Given this increase in MMP9, as well as previous studies demonstrating that targeted reduction of KLF6-SV1 reduces cellular migration and invasion in both prostate and ovarian cancer cell lines (ref. 15 and our unpublished observations), we directly examined the effect of KLF6-SV1 overexpression on invasion. Consistent with these previous findings, overexpression resulted in increased cellular invasion (Figure 2D).

KLF6-SV1 increases metastasis in vivo, but not localized tumor growth. To further explore the relevance of increased KLF6-SV1 expression in vivo, we used an orthotopic model of PCa progression, combining PC3 cell lines stably engineered to express both the firefly luciferase gene and KLF6-SV1 and whole-body bioluminescent imaging (BLI). This model allows for in vivo monitoring of local tumor growth and dissemination in real time (21). Prior to intraprostatic injection, the average bioluminescence of these cell lines was determined and shown to be directly proportional to cell number, and the luminescent signals emitted by both cell lines were similar (Supplemental Figure 1; supplemental material available online with this article; doi:10.1172/JCI34780DS1). After orthotopic surgical implantation of either pBABE vector– or pSV1 vector–expressing PC3 cells, SCID mice were imaged weekly to compare prostatic signal intensity and to monitor for the development of regional metastasis. No significant differences between intraprostatic tumor growth between the 2 experimental groups were identified (Figure 3A).

Striking differences were noted, however, with regard to the development of metastases. In the KLF6-SV1–expressing PC3 group, the time to metastatic development was shorter, and both the total number of metastatic sites and the size of the resultant tumor foci was significantly higher than in controls (Figure 3B and Table 1). Ex vivo imaging and histology was performed on the metastatic lesions from a subset of these mice (Figure 3C). The increased metastatic potential and burden of KLF6-SV1–overexpressing cells was associated with decreased expression of p21 and the proapoptotic, BH3-only family member NOXA in vivo (Figure 3D). Together, these data suggest that increased expression of KLF6-SV1 promotes metastasis in vivo while not affecting local tumor growth. These findings are consistent with the gene expression, tissue microarray, and clinicopathologic association data demonstrating increased KLF6-SV1 expression in hormone-refractory metastatic PCa and in aggressive localized tumors with a high propensity to develop recurrence after radical prostatectomy.

KLF6-SV1 overexpression increases PCa dissemination. An intracardiac model of metastasis was then used to further explore the biological and/or functional role of KLF6-SV1 in PCa dissemination. In contrast to the intraprostatic system, which models local growth and invasion, the intracardiac model recapitulates the late steps in PCa metastasis, specifically tumor cell dissemination, survival, invasion, colonization, and distant growth (22). Mice were imaged immediately after injection to confirm whole-body distribution secondary to successful introduction of the cells into the left ventricle (Figure 4A). Strikingly, all mice injected with KLF6-SV1–overexpressing PC3 cells (8 of 8) had evidence of distant tumor cell colonization and growth at 13 d, whereas 35% (3 of 8) of the control pBABE vector–expressing PC3 cells showed evidence of metastatic growth at this time point ($P < 0.01$; Figure 4B). The median time to metastatic development was more than 3.5 times greater in the control mice (24 d; $P < 0.009$). In addition to differences in time to metastatic colonization, the bioluminescent signals (and thus the size of resultant tumor masses) from KLF6-SV1–expressing PC3 metastatic lesions were 3 orders of magnitude higher than those of control pBABE vector–expressing PC3 cell–injected mice (Figure 4A). The increased growth of these metastatic colonies is also notable given the lack of measurable growth differences observed after intraprostatic implantation (Figure 3A).

Ex vivo imaging and histology was performed on 20 different tissues excised from a subset of mice after final in vivo imaging (Figure 4C and Table 2). Overexpression of KLF6-SV1 in vivo not only led to decreased time to metastasis and increased metastatic burden, but also resulted in significantly increased metastases to specific tissue sites; metastases were twice as frequent to lymph nodes and bone in these mice (Table 2). Moreover, brain metastases were identified only in the KLF6-SV1 group, not in the control group.

KLF6-SV1 expression affects proliferation, angiogenesis, and apoptosis in vivo. We next explored potential mechanisms underlying KLF6-SV1–mediated increases in invasion, metastasis, and dissemination in both the intraprostatic and intracardiac models. The expression pattern of markers of cell proliferation (proliferating cell nuclear antigen [PCNA]), angiogenesis (CD31; also known as PECAM1), and apoptosis (TUNEL) were examined in metastatic KLF6-SV1–derived tumors. Immunohistochemistry showed increased PCNA staining in KLF6-SV1–derived tumors ($P < 0.01$; Figure 5A). Tumor growth in vivo is known to be dependent on the ability of cancer cells to stimulate blood vessel growth through upregulation of angiogenic mediators. CD31 is highly expressed by endothelial cells and is a reproducible marker of angiogenesis in transplanted tumor models (23). KLF6-SV1–derived tumors demonstrated a

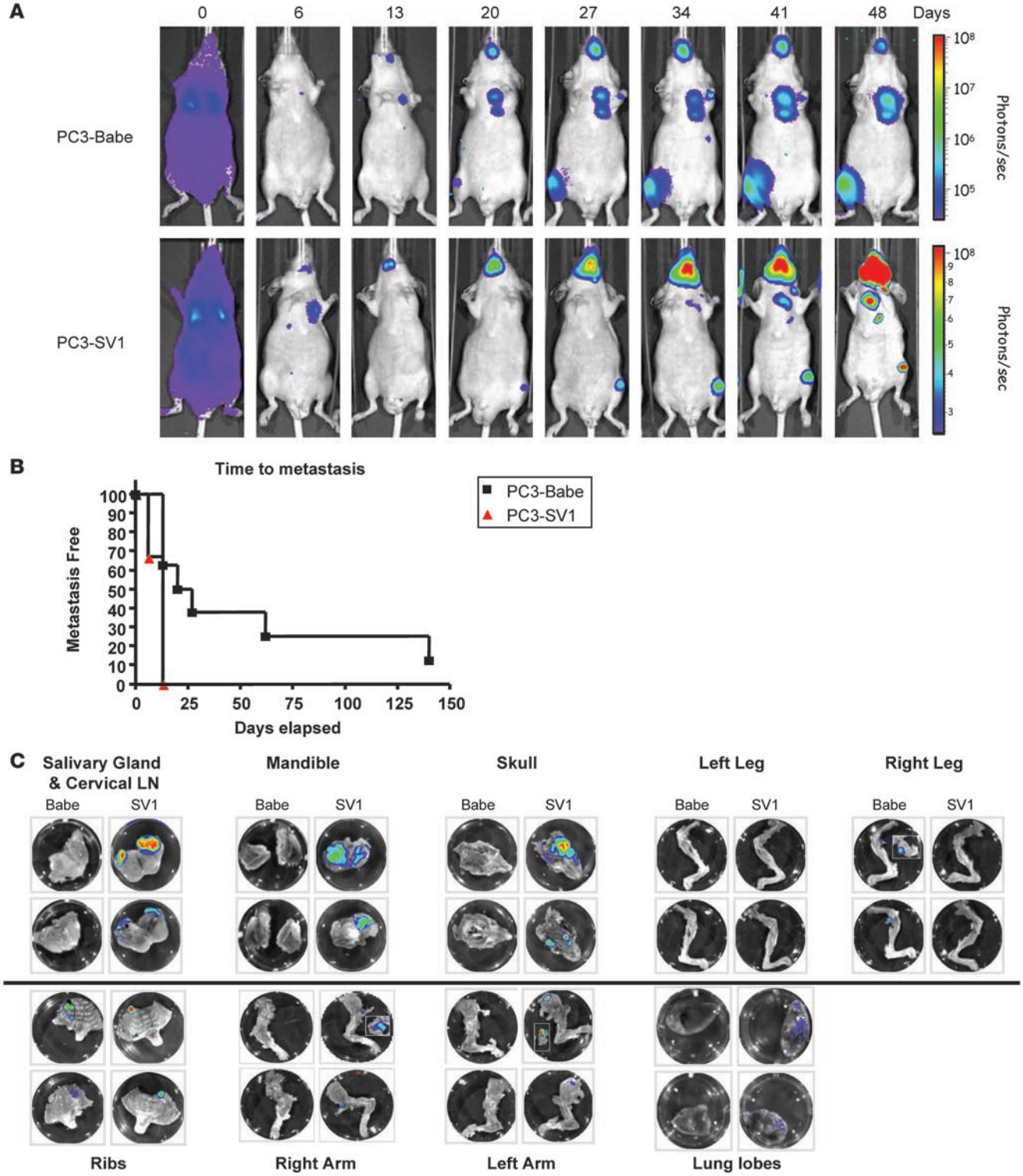

Figure 4

Intracardiac model of PCa dissemination and metastasis. (**A**) Female *nu/nu* mice were injected with 1×10^6 PC3 cells in 25 μl PBS. In vivo BLI was performed weekly 10–15 minutes after animals received the substrate D-luciferin at 150 mg/kg in PBS by i.p. injection. The bioluminescent signals from metastatic lesions in the KLF6-SV1–expressing PC3 cell group was 3 orders of magnitude higher than the control pBABE vector–expressing PC3 cell–injected mice, demonstrating that the former developed larger metastatic tumors. (**B**) pSV1 vector–expressing cells demonstrated detectable metastasis significantly earlier than did control pBABE vector–expressing cells lines ($P < 0.01$). The median time to metastatic development was 3.5 times more rapid in the mice with KLF6-SV1–expressing PC3 cells (7 d) compared with controls (24 d; $P < 0.009$). (**C**) Ex vivo imaging and histology was performed on 20 different tissues excised from a subset of mice after final in vivo imaging. Representative images are shown.

Table 2
KLF6-SV1–overexpressing cells display tissue tropism different from that of control cells

	pBABE	pBABE-SV1
Lymph node	28%	55%[A]
Bone	12%	29%[B]
Visceral organ	16%[A]	0%
Brain	0%	13%[A]
Other sites	0%	17%[A]
Total metastases	16%	36%[B]

All metastatic sites were determined at time of sacrifice, counted for each mouse, and summarized. Values represent tumor incidence. Overexpression of KLF6-SV1 resulted in different sites of dissemination, including increased numbers of bone, lymph nodes, and brain metastases. [A]$P < 0.01$. [B]$P < 0.001$.

nearly 4-fold increase in CD31 staining, consistent with increased angiogenesis ($P < 0.01$; Figure 5B). TUNEL staining of pBABE vector– and KLF6-SV1–derived tumors demonstrated a 70% reduction in apoptotic cells in KLF6-SV1–overexpressing tumors compared with controls ($P < 0.01$; Figure 5C).

Targeted reduction of KLF6-SV1 results in spontaneous apoptosis and decreased tumor growth. Given these findings, and to establish proof-of-concept of targeted treatment, we examined the biological effect of KLF6-SV1 inhibition on PCa development and progression in both cell culture and in vivo model systems using siRNA. Transient transfection of a chemically modified KLF6-SV1–specific siRNA (si-SV1) in PC3M cell lines resulted in a 60% or greater decrease in KLF6-SV1 protein levels (Figure 6A). Targeted downregulation of KLF6-SV1 was associated with a 4- to 6-fold increase in spontaneous apoptosis, as shown by the percentage of sub-G1 cells by fluorescence-activated cell sorting analysis (Figure 6B). These changes were associated with increased poly(ADP-ribose) polymerase (PARP) cleavage and active caspase-3 and -8 expression (Figure 6C). qRT-PCR was used to determine whether the proapoptotic NOXA and antiapoptotic Bcl-2 were regulated by KLF6-SV1, as we have noted in other experiments (our unpublished observations). Consistent with our recent findings in ovarian cancer (A. DiFeo and J.A. Martignetti, unpublished observations), NOXA mRNA expression was increased 6-fold in cell lines transfected with si-SV1 compared with control, while Bcl-2 expression was reduced 80% in this same experiment, at both the mRNA and protein levels (Figure 6D).

Intratumoral injection of siRNA has been used to successfully target specific cancer-relevant pathways in a number of tumor xenograft models (24). We were therefore interested in examining the potential therapeutic role of targeted reduction of KLF6-SV1 in an established prostate tumor model. We injected PC3M into nude mice and allowed subcutaneous tumors to form for 3 weeks prior to direct intratumoral injection (3 mg/kg) of either si-SV1 or nontargeting control siRNA (si-NTC) twice a week for 3 weeks. Tumors were measured twice a week, prior to each treatment. During the experimental time course, si-SV1–treated tumors were markedly growth inhibited compared with si-NTC–treated tumors ($P < 0.01$; Figure 7, A and B).

Mice were sacrificed at the end of the study, and tumors were excised for both RNA and immunohistochemical analysis. Real-time PCR analysis confirmed that si-SV1–treated tumors had a greater than 60% reduction in KLF6-SV1 mRNA levels compared with control-injected tumors, while no differences were noted in KLF6 mRNA levels (data not shown). On average, si-SV1–treated tumors decreased approximately 80% in size compared with con-

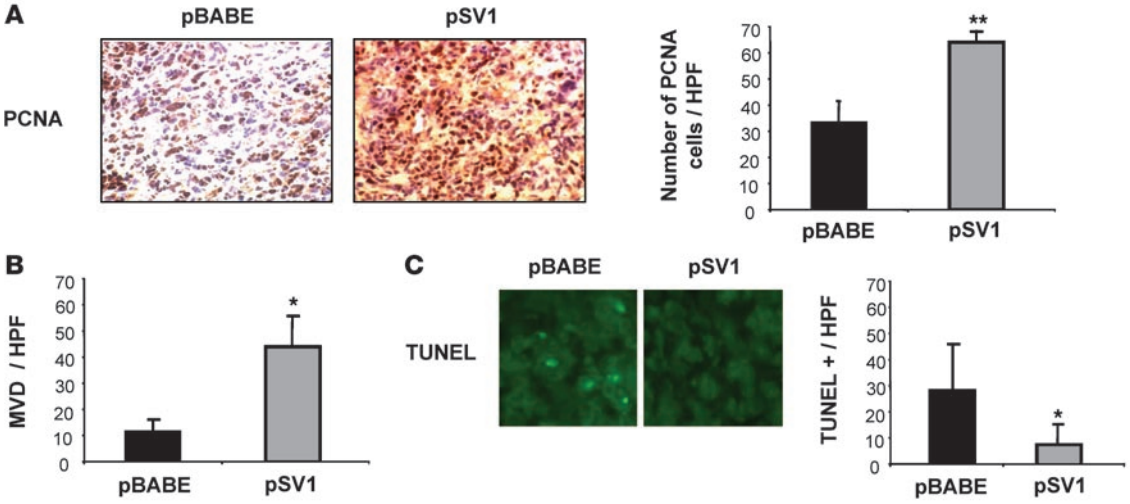

Figure 5
Changes in KLF6-SV1 metastatic tumor behavior correlates with markers of cellular proliferation, angiogenesis, and apoptosis. Metastatic tumors were analyzed for their expression of PCNA, CD31, and TUNEL. (**A**) Immunohistochemistry for PCNA in pBABE vector– and KLF6-SV1–derived tumors. KLF6-SV1 caused increased PCNA staining in vivo. Eight independent high-power fields for each pBABE ($n = 4$) and KLF6-SV1 ($n = 6$) tumor were counted, assessing both the total number of cells and PCNA-positive cells. The graph represents the average percentage of PCNA-positive cells for each group. (**B**) CD31 staining of pBABE and KLF6-SV1 cell line–derived tumors. Overexpression of KLF6-SV1 protein caused a 4-fold increase in microvessel density (MVD), as measured by the number of CD31-positive endothelial cells per ×400 high-power field (HPF). (**C**) TUNEL staining of pBABE and KLF6-SV1 tumors. Representative images are shown. Overexpression of KLF6-SV1 decreased apoptosis by 70%. For each tumor, 6 high-power fields were counted and the total number of TUNEL-positive cells was determined. *$P < 0.01$, **$P < 0.001$ versus control. Original magnification, ×400.

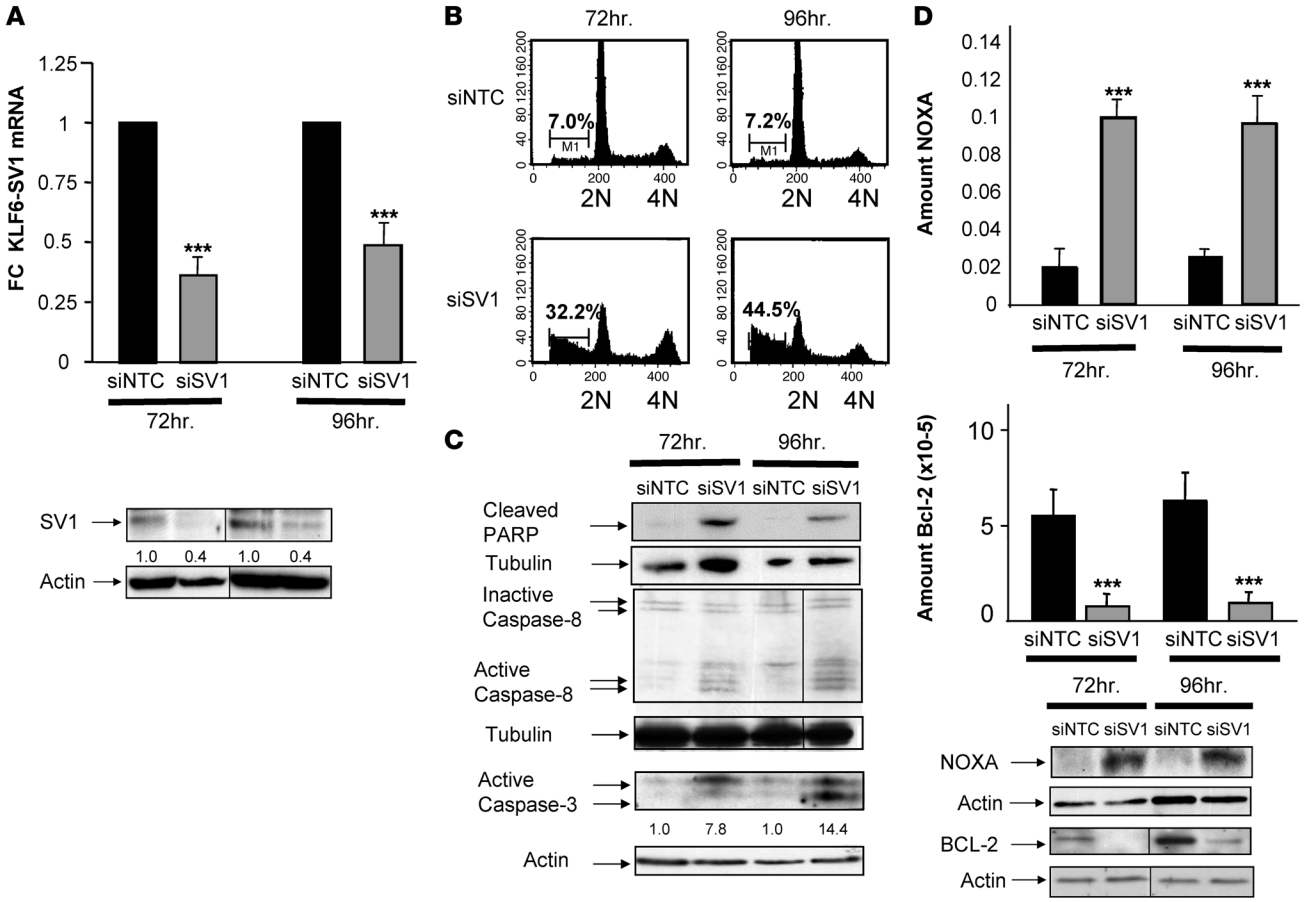

Figure 6

Targeted KLF6-SV1 inhibition dramatically increases spontaneous apoptosis. (**A**) qRT-PCR and Western blot analysis of the PC3M cell line transfected with si-NTC and si-SV1 demonstrated significant downregulation of KLF6-SV1 mRNA and protein at 72 and 96 h. (**B**) Fluorescence-activated cell sorting analysis of si-NTC– and si-SV1–transfected PC3 cells at 72 and 96 h. On average, si-SV1 treatment increased cell death 5-fold. Data represent the average of 3 independent experiments. Numbers within plots indicate percent hypodiploid (i.e., apoptotic) cells. (**C**) Western blot analysis demonstrated marked upregulation of caspase-3 and -8 and increased poly(ADP-ribose) polymerase (PARP) cleavage in si-SV1–transfected cell lines. (**D**) qRT-PCR and Western blot analysis of si-NTC– and si-SV1–transfected cells for NOXA and Bcl-2 demonstrated marked upregulation of the proapoptotic NOXA with concomitant downregulation of Bcl-2. Numbers above actin blots in **A** and **C** represent densitometric analysis of the protein bands, expressed as fold change relative to control and normalized to actin. In **A**, **B**, and **D**, lanes were run on the same gel but were noncontiguous (black lines). Each Western blot shown is representative of 3 independent experiments. ***$P < 0.0001$ versus control.

trol-treated tumors (Figure 7B). A significant increase in apoptosis was evident in si-SV1–treated tumors in vivo (Figure 7C), and these tumors had half the levels of Bcl-2 and 3 times the NOXA than did controls (Figure 7D).

Discussion

Metastasis represents one stage in the evolution of cancer cells wherein a sequential series of interrelated steps — including invasion, intravasation, transport through the circulation, arrest, extravasation, and growth at secondary sites — results in nearly all human cancer-related deaths (25, 26). Current attempts to define the molecular events associated with or leading to this cascade have most notably resulted in gene expression profiles mediating tissue-specific breast cancer metastasis to bone (27) and lung (28). In turn, these molecular profiles share a relationship with those that are clinically predictive of breast cancer outcome and survival (29, 30). While a metastatic gene signature common to multiple tumor types has also been identified (31), in general, these successes in identifying clinically relevant signatures and key genetic determinants that regulate tumor cell dissemination, tissue-specific homing of cells, and metastatic implantation and growth of circulating tumor cells have not yet been fully duplicated in PCa. Our studies demonstrate a functional link, namely the propensity for increased metastatic spread, by which KLF6-SV1 overexpression is associated with decreased patient survival and disease recurrence in PCa.

PCa remains the second leading cause of cancer-related death in the United States, and treating this disease remains a diagnostic dilemma. While early-stage disease is treatable, with a 5-year survival rate exceeding 80%, nearly 30% of men treated by radical prostatectomy will relapse, and the prognosis for men with metastatic PCa remains poor (32). Androgen ablation therapy is one of the most commonly used therapies in the treatment of advanced metastatic PCa (33), but while most patients initially respond to this therapy, most ultimately relapse and die from androgen-independent PCa and metastasis (33). The clinical

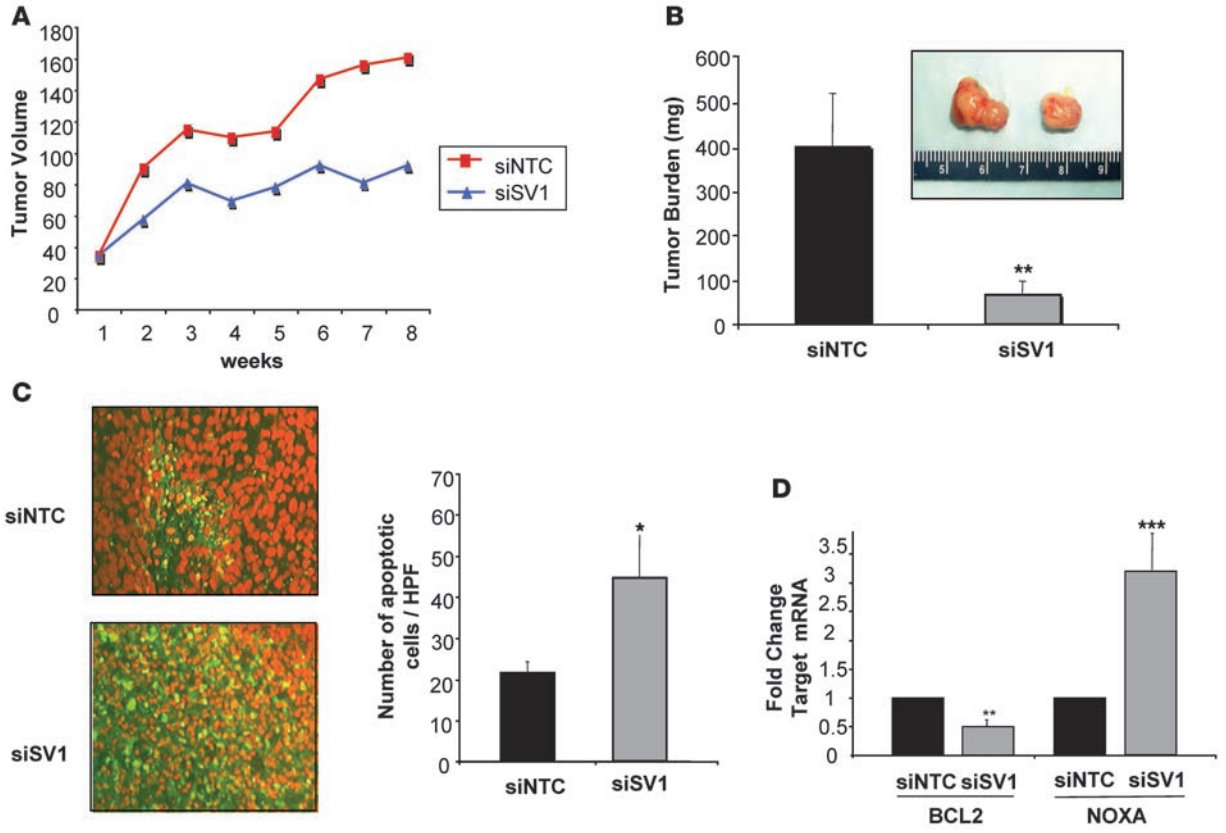

Figure 7

Direct intratumoral injection of si-SV1 induces apoptosis and reduces tumor growth in vivo. (**A**) Intratumoral injection of si-SV1 reduced tumor growth in a PCa xenograft model. PC3M cells were injected subcutaneously into nude mice. After 3 weeks of growth, mice were randomized into 2 treatment groups, and si-NTC or si-SV1 was injected directly into the tumors twice a week for a total of 3 weeks. Mice were sacrificed, tumor volume was determined, and RNA and tissue was harvested. (**B**) Photographs of representative si-NTC– and si-SV1–treated tumors, which had identical volumes prior to treatment. Three weeks after treatment, si-SV1–injected tumors were significantly smaller than si-NTC–treated tumors. $n = 9$ (si-SV1); 8 (si-NTC). (**C**) TUNEL staining of si-SV1– and si-NTC–treated tumors revealed a significant increase in the number of apoptotic cells per high-power field in si-SV1–derived tumors. Six tumors per high-power field were counted. (**D**) qRT-PCR of si-NTC ($n = 7$) and si-SV1 ($n = 8$) derived tumors using PCR primers specific to human Bcl-2 and NOXA demonstrate a 50% reduction in Bcl-2 expression with a concomitant 3 fold increase in NOXA expression in si-SV1 treated tumors. *$P < 0.01$, **$P < 0.001$, ***$P < 0.0001$ versus control. Original magnification, ×400.

challenge remains correctly identifying and stratifying those with higher and lower risks of relapse and defining the pathways responsible for these biologic differences.

In this study, we specifically analyzed the mechanism by which a single gene, from a multigene signature in several independent studies examining clinical outcome (11, 12, 16) and late-stage disease in PCa (34), affects PCa cell behavior. In this sense, these gene expression profiling studies served a hypothesis-generating role for KLF6-SV1. Our results demonstrated that KLF6-SV1 was upregulated in hormone-refractory metastatic PCa, and its increased expression was predictive of poor survival and disease recurrence in primary PCa. Intriguingly, while overexpression of KLF6-SV1 resulted in increased metastasis and tumor cell dissemination to lymph nodes, bone, and brain, this metastatic behavior was independent of an effect on local growth. These findings are in keeping with the theory that tumor formation and metastasis are distinct processes. Thus, KLF6-SV1, which is alternatively spliced from the tumor suppressor KLF6, seems to function as a metastasis promoter gene. We adopt this term based on KLF6-SV1's contrasting role to metastasis suppressors, which block tumor cell metastasis at distant, but not primary, sites by blocking different stages of the metastatic cascade (35).

We additionally demonstrated that KLF6-SV1 overexpression resulted in marked changes in 3 key pathways regulating tumor growth and dissemination: apoptosis, cellular proliferation, and angiogenesis. Each is believed to play a critical role in tumor growth and metastasis. Therefore, inhibition of KLF6-SV1 theoretically represents an intriguing therapeutic target, because multiple pathways would be inhibited simultaneously. Even alone, the apoptotic pathway may represent a highly relevant target in treatment, because resistant tumor cells are believed to have a distinct advantage in surviving the relatively inefficient steps required to successfully establish a metastatic tumor focus (36). The results of our present study, combined with our recent findings that KLF6-SV1 is an antiapoptotic protein that binds and targets the proapoptotic Bcl-2 family member NOXA for degradation and that KLF6-SV1 inhibition in vivo can prolong survival in a disseminated ovarian cancer model (A. DiFeo and J.A. Martignetti, unpublished observations), suggests that KLF6-SV1 inhibition could also represent a novel therapeutic strategy in PCa.

Methods

Cell culture and cell line generation. All cell lines were obtained from the American Tissue Culture Collection. Luciferase-expressing stable cell lines were obtained from J. Blanco (Centro de Investigacion Cardiovascular, Barcelona, Spain). Retroviral infection with wild-type KLF6 and KLF6-SV1 was performed as follows. Stable cell lines were generated by retroviral infection of SKOV3 cells with either a control virus (pBABE) or KLF6-SV1 (pSV1). For standard infection, approximately 1×10^6 viral particles were incubated with 5×10^5 SKOV3 cells in a final volume of 2 ml in the presence of Polybrene (4 μg/ml) for 5 h. Infected cells were then subjected to selection in puromycin (4 μg/ml), and a mass population of selected cells was used for subsequent analysis.

PCa sample collection. Tissue samples were obtained from 62 patients with clinically localized prostate carcinoma treated by radical prostatectomy alone at Memorial Sloan-Kettering Cancer Center between 1993 and 1999. Sixty-two tissue samples from patients with 3 consecutive PSA increases greater than 0.1 ng/ml were classified as recurrent disease. Twenty-nine tissue samples from patients with an undetectable PSA level for 5 years (range, 60–108 months) were classified as nonrecurrent. As determined by the range of postoperative nomogram predictions, the patients in our cohort represented a broad spectrum of disease severity. Tissue samples were snap-frozen in liquid nitrogen and stored at –80°C. Each tissue sample was examined histologically using H&E-stained cryostat sections. The frozen blocks were manually trimmed to enrich for neoplastic epithelium with minimal contamination from benign epithelial and stromal elements. All studies were approved by the institutional review boards of the Memorial Sloan-Kettering Cancer Center and Brigham and Women's Hospital. Informed consent was obtained from all subjects.

We prespecified the hypothesis that a high level of KLF6-SV1 was a negative prognostic indicator of survival. The samples, all reviewed by a single investigator, were selected to enrich for biochemical recurrence so that there were enough events to evaluate. The full description of the sample set has been previously published (37). For determination of sample size, see *Statistics*.

Array analysis. Complementary DNA microarray analysis of gene expression was done essentially as described previously (16). The Oncomine database (http://www.oncomine.org/) was also used to assess KLF6 expression in the prostate cancer microarray data set (16). Primary analysis was done with the Genepix pro 4.0 software package (Molecular Devices). Cy3/Cy5 ratios were determined for KLF6, along with various other quality control parameters (e.g., intensity over local background). The normalized median of ratio values of the KLF6 gene was $\log_2$ transformed, filtered for presence across arrays, and selected for expression levels and patterns depending on the experimental set as stated in the figure legends. Figures were generated with TreeView software (version 1.60).

Migration and invasion assays. Standard invasion assays were performed as we have previously described (15). Briefly, assays were performed in Boyden chambers using a reconstituted basement membrane (Matrigel, 0.5 mg/ml; BD). Coated membranes were first blocked with 0.5% BSA in DMEM and equilibrated in 0.1% BSA in DMEM. Approximately 10^5 cells in serum-free DMEM were added to the upper chamber, and conditioned medium derived from NIH 3T3 fibroblasts was used in the lower chamber as a chemoattractant. After incubation for 19 h at 37°C, cells in the upper chamber were thoroughly removed by gentle suctioning. Cells that invaded the barrier were fixed in 10% formalin and stained with 4′,6-diamidino-2-phenylindole in PBS. Nuclei were visualized under a fluorescence microscope, and 5 randomly selected nonoverlapping fields were imaged and counted.

Intratumoral injection. PC3M cells (1×10^6) were injected into the left flank of female 6- to 8-week-old BALB/c *nu/nu* mice. Three weeks after inoculation, when the tumors had reached an average volume of 150–200 mm^3, 5 nmol/kg si-NTC or si-SV1 was injected directly into the tumor using a 28.5-gauge syringe (BD). Tumor volumes were measured twice weekly and calculated as length × width × width × 0.4. Intratumoral tumor injections were repeated twice weekly for 3 weeks, at which time the mice were sacrificed and the tumors were excised for RNA analysis.

Densitometric analysis. Enhanced chemiluminescent images of immunoblots were analyzed by scanning densitometry and quantified with a Bioquant NOVA imaging system and Bioquant NOVA PRIME software. All values were normalized to actin and expressed as fold change relative to control.

Western blot analysis. Cell extracts for Western blotting were harvested in radioimmunoprecipitation assay buffer (Santa Cruz Biotechnology Inc.) according to standard protocols. Tumor tissue extracts were harvested and prepared in T-PER reagent (Pierce). Equal amounts of protein (50 μg) — as determined by the Bio-Rad DC Protein quantification assay — were loaded, separated by PAGE, and transferred to nitrocellulose membranes. Western blotting was done using a goat polyclonal antibody to actin and c-myc (SC-1616 and SC-6458, respectively; Santa Cruz Biotechnology Inc.) as well as monoclonal antibodies to p21 (Santa Cruz Biotechnology Inc.) and the KLF6 2A2 and 9A2 antibodies (Zymed).

Analysis of proliferation. Proliferation was determined by estimating [^{3}H]thymidine incorporation. PC3M stable cell lines expressing pBABE and pBABE-SV1 vectors were plated at a density of 50,000 cells/well in 12-well dishes. At 48 h after plating, 1 μCi/ml [^{3}H]thymidine (Amersham) was added. After 2 h, cells were washed 4 times with ice-cold PBS and fixed in methanol for 30 minutes at 4°C. After methanol removal and cell drying, cells were solubilized in 0.25% sodium hydroxide and 0.25% SDS. After neutralization with hydrochloric acid (1 N), disintegrations per minute were estimated by liquid scintillation counting.

RNA and qRT-PCR analysis. Normal, BPH, and PCa RNA samples were collected and extracted as previously described (16). Cell line and tumor RNA was extracted using the RNeasy Mini and Midi kit (Qiagen). All RNA was treated with DNAse (Qiagen). A total of 1 mg RNA was reverse transcribed per reaction using first strand complementary DNA synthesis with random primers (Promega). RT-PCR was performed with KLF6 5′ and 3′ untranslated region–specific primers on 10 ng cDNA derived from normal, localized, and metastatic PCa as previously described (14). qRT-PCR was performed using the PCR primers previously described (14) on an ABI PRISM 7900HT Sequence Detection System (Applied Biosystems). All experiments were done in triplicate and independently validated 3 times. All values were normalized to GAPDH levels. KLF6 alternative splicing was determined as previously described (14, 15).

BLI. In vitro and in vivo BLI was performed with an IVIV Imaging System (Xenogen). Images and measurements of bioluminescent signals were acquired and analyzed using Living Image and Xenogen software. At 15 min prior to imaging, animals received the substrate D-luciferin at 150 mg/kg in Dulbecco PBS (DPBS) with 0.5% BSA by i.p. injection and were anesthetized using 3% isoflurane. Imaging time ranged from 1 to 5 min, depending on the signal emitted from each mouse, and 5 mice were imaged at a time. The light emitted from the tumors in each mouse was detected and quantified.

Intracardiac metastasis model. Male *nu/nu* mice (6–8 weeks of age) were anesthetized using 20 mg/kg ketamine hydrochloride and 6 mg/kg xylazine prior to injection of 3×10^6 PC3-luc-empty or PC3-luc-SV1 cells suspended in 100 μl DPBS into the left ventricle of the heart (21, 23). Mice were then imaged after 1 h to confirm successful intracardiac injection, showing systemic bioluminescence distributed throughout the mouse. Only mice with evidence of a satisfactory injection were used for analysis. The development of metastasis was monitored once a week in vivo by BLI until the mice succumbed to the disease. Upon necropsy, all organs were excised and prepared for ex vivo imaging and subsequent histopathology analysis.

Orthotopic prostate model. Male *nu/nu* mice (6–8 weeks of age) were anesthetized using 120 mg/kg ketamine hydrochloride plus 6 mg/kg xylazine and surgically injected with 5×10^5 of either PC3-luc-empty or PC3-luc-SV1 suspended in 30 μl DPBS into the dorsolateral prostate lobes. One week after injection, surgical staples were removed, and mice were imaged as described above. Prostate tumor growth and local metastasis was monitored weekly using BLI.

Histopathology. To confirm the presence of neoplastic cells, selected tissues samples were preserved in 10% formalin and prepared for histological analysis. Tissue sections were stained with H&E, factor VII, PCNA, or TUNEL. Immunohistochemical staining for factor VIII–related antigen and PCNA were carried out as previously described (15) using a factor VIII–related antigen (DAKO) antibody for the detection of tumor microvessel density, a PCNA antibody (Santa Cruz Biotechnology Inc.) for the detection of tumor cell proliferation, and TUNEL staining (Roche) for apoptosis. Measurements of PCNA and TUNEL staining and microvessel density were done as previously described (15). Briefly, microvessels that stained positive for factor VIII–related antigen were counted on 4 representative high-power fields (magnification, ×400) for each tumor. Data were expressed as the average number of microvessels per high-power field for each experimental tumor group. PCNA staining was determined by counting the number of positive cells per high-power field and dividing that number by the total number of cells in that particular field. For each tumor, 6 high-power fields were counted, and the average for each experimental tumor group was determined.

Statistics. A multivariate survival analysis was performed using a Cox proportional hazards model, which considered KLF6-SV1 a continuous variable. The statistical plan included a traditional sample size calculation using classical criteria: significance, 0.05; power, 0.8; 2-sided testing; and a relative risk estimate based on previously published data (11). This resulted in an estimated sample size of 70 to determine differences in biochemical recurrence and KLF6-SV1 expression. ANOVA with the Tukey post-hoc test was used for comparisons of continuous variables. Univariate survival rate analyses were estimated using the Kaplan-Meier method, with comparisons made between groups by the log-rank test. All statistical analyses were conducted using SAS 9.1 (SAS Institute Inc.). Statistical significance was assumed for a 2-tailed *P* value less than 0.05. Data are presented as mean ± SD unless otherwise indicated.

Acknowledgments

This work was funded by NIH grants DK37340 (to S.L. Friedman), U01 CA84999 and P50 CA92629 (to W. Gerald), RO1 CA125612 (to M.A. Rubin), and CA122332 (to J.A. Martignetti) and by a Prostate Cancer Foundation Award to J.A. Martignetti. We thank Yu Zhou of the In Vivo Molecular Imaging Lab at the Mount Sinai School of Medicine for his technical support. We also thank Jeronimo Blanco for providing the PC3-luc cells.

Received for publication December 17, 2007, and accepted in revised form April 23, 2008.

Address correspondence to: John A. Martignetti, Mount Sinai School of Medicine, 1425 Madison Avenue, Room 14-70, New York, New York 10029, USA. Phone: (212) 659-6744; Fax: (212) 849-2638; E-mail: john.martignetti@mssm.edu.

Goutham Narla and Analisa DiFeo are co-first authors.

1. Jemal, A., et al. 2007. Cancer statistics, 2007. *CA Cancer J. Clin.* **57**:43–66.
2. Narla, G., et al. 2001. KLF6, a candidate tumor suppressor gene mutated in prostate cancer. *Science.* **294**:2563–2566.
3. Chen, C., et al. 2003. Deletion, mutation, and loss of expression of KLF6 in human prostate cancer. *Am. J. Pathol.* **162**:1349–1354.
4. Reeves, H.L., et al. 2004. Kruppel-like factor 6 (KLF6) is a tumor-suppressor gene frequently inactivated in colorectal cancer. *Gastroenterology.* **126**:1090–1103.
5. Kremer-Tal, S., et al. 2004. Frequent inactivation of the tumor suppressor kruppel-like factor 6 (KLF6) in hepatocellular carcinoma. *Hepatology.* **40**:1047–1052.
6. Chen, H.K., et al. 2002. Mutation analysis of KLF6 gene in human nasopharyngeal carcinomas. *Ai Zheng.* **21**:1047–1050.
7. Jeng, Y.M., and Hsu, H.C. 2003. KLF6, a putative tumor suppressor gene, is mutated in astrocytic gliomas. *Int. J. Cancer.* **105**:625–629.
8. Yamashita, K., et al. 2002. Pharmacologic unmasking of epigenetically silenced tumor suppressor genes in esophageal squamous cell carcinoma. *Cancer Cell.* **2**:485–495.
9. Kettunen, E., et al. 2004. Differentially expressed genes in nonsmall cell lung cancer: Expression profiling of cancer-related genes in squamous cell lung cancer. *Cancer Genet. Cytogenet.* **149**:98–106.
10. Ito, G., et al. 2004. Kruppel-like factor 6 is frequently down-regulated and induces apoptosis in non-small cell lung cancer cells. *Cancer Res.* **64**:3838–3843.
11. Glinsky, G.V., Glinskii, A.B., Stephenson, A.J., Hoffman, R.M., and Gerald, W.L. 2004. Gene expression profiling predicts clinical outcome of prostate cancer. *J. Clin. Invest.* **113**:913–923.
12. Singh, D., et al. 2002. Gene expression correlates of clinical prostate cancer behavior. *Cancer Cell.* **1**:203–209.
13. Macleod, K., et al. 2005. Altered ErbB receptor signaling and gene expression in cisplatin-resistant ovarian cancer. *Cancer Res.* **65**:6789–6800.
14. Narla, G., et al. 2005. A germline DNA polymorphism enhances alternative splicing of the KLF6 tumor suppressor gene and is associated with increased prostate cancer risk. *Cancer Res.* **65**:1213–1222.
15. Narla, G., et al. 2005. Targeted inhibition of the KLF6 splice variant, KLF6 SV1, suppresses prostate cancer cell growth and spread. *Cancer Res.* **65**:5761–5768.
16. Dhanasekaran, S.M., et al. 2001. Delineation of prognostic biomarkers in prostate cancer. *Nature.* **412**:822–826.
17. Benzeno, S., et al. 2004. Cyclin-dependent kinase inhibition by the KLF6 tumor suppressor protein through interaction with cyclin D1. *Cancer Res.* **64**:3885–3891.
18. Slavin, D.A., et al. 2004. A new role for the kruppel-like transcription factor KLF6 as an inhibitor of c-jun proto-oncoprotein function. *Oncogene.* **23**:8196–8205.
19. Kimmelman, A.C., et al. 2004. Suppression of glioblastoma tumorigenicity by the kruppel-like transcription factor KLF6. *Oncogene.* **23**:5077–5083.
20. DiFeo, A., et al. 2006. E-cadherin is a novel transcriptional target of the KLF6 tumor suppressor. *Oncogene.* **25**:6026–6031.
21. Lyons, S.K., et al. 2006. Noninvasive bioluminescence imaging of normal and spontaneously transformed prostate tissue in mice. *Cancer Res.* **66**:4701–4707.
22. Drake, J.M., Gabriel, C.L., and Henry, M.D. 2005. Assessing tumor growth and distribution in a model of prostate cancer metastasis using bioluminescence imaging. *Clin. Exp. Metastasis.* **22**:674–684.
23. Shih, S.C., et al. 2002. Molecular profiling of angiogenesis markers. *Am. J. Pathol.* **161**:35–41.
24. Xie, F.Y., Woodle, M.C., and Lu, P.Y. 2006. Harnessing in vivo siRNA delivery for drug discovery and therapeutic development. *Drug Discov. Today.* **11**:67–73.
25. Fidler, I.J. 2003. The pathogenesis of cancer metastasis: the 'seed and soil' hypothesis revisited. *Nat. Rev. Cancer.* **3**:453–458.
26. Steeg, P.S. 2006. Tumor metastasis: mechanistic insights and clinical challenges. *Nat. Med.* **12**:895–904.
27. Kang, Y., et al. 2003. A multigenic program mediating breast cancer metastasis to bone. *Cancer Cell.* **3**:537–549.
28. Minn, A.J., et al. 2005. Genes that mediate breast cancer metastasis to lung. *Nature.* **436**:518–524.
29. van 't Veer, L.J., et al. 2002. Gene expression profiling predicts clinical outcome of breast cancer. *Nature.* **415**:530–536.
30. van de Vijver, M.J., et al. 2002. A gene-expression signature as a predictor of survival in breast cancer. *N. Engl. J. Med.* **347**:1999–2009.
31. Ramaswamy, S., Ross, K.N., Lander, E.S., and Golub, T.R. 2003. A molecular signature of metastasis in primary solid tumors. *Nat. Genet.* **33**:49–54.
32. Sooriakumaran, P., Khaksar, S.J., and Shah, J. 2006. Management of prostate cancer. Part 2: localized and locally advanced disease. *Expert Rev. Anticancer Ther.* **6**:595–603.
33. Bhandari, M.S., Petrylak, D.P., and Hussain, M. 2005. Clinical trials in metastatic prostate cancer — has there been real progress in the past decade? *Eur. J. Cancer.* **41**:941–953.
34. Stanbrough, M., et al. 2006. Increased expression of genes converting adrenal androgens to testosterone in androgen-independent prostate cancer. *Cancer Res.* **66**:2815–2825.
35. Rinker-Schaeffer, C.W., O'Keefe, J.P., Welch, D.R., and Theodorescu, D. 2006. Metastasis suppressor proteins: discovery, molecular mechanisms, and clinical application. *Clin. Cancer Res.* **12**:3882–3889.
36. Mehlen, P., and Puisieux, A. 2006. Metastasis: a question of life or death. *Nat. Rev. Cancer.* **6**:449–458.
37. Stephenson, A.J., et al. 2005. Integration of gene expression profiling and clinical variables to predict prostate carcinoma recurrence after radical prostatectomy. *Cancer.* **104**:290–298.